

**FRACTURE PHENOMENA IN SODA LIME SILICA GLASS  
CAUSED BY BULLET IMPACTS**

**by**

**SHARIFAH MASTURA BT SYED MOHD DAUD**

**Thesis submitted in fulfillment of the requirements  
for the degree of  
Master of Science**

**February 2012**

## ACKNOWLEDGEMENTS

I would like to take this opportunity to acknowledge many people who have been involved directly and indirectly in this study. First of all, my deepest appreciation goes to my main supervisor, Assoc. Prof. Dr. R. Kuppuswamy for all of his help and guidance during the research. I am much thankful for his continuous support, professional guidance, encouragement, and patience throughout my study. I would also like to thank my co-supervisors, Assoc. Prof. Dr. Sharifah Mastura Syed Mohamad and Dr. Mohammad Hadzri Yaacob for their advice, encouragement, time, advice and critique of my thesis. Special thanks are expressed to Professor R. Jagannathan, Chennai Mathematical Institute, India for his advice to apply fractal dimensions to analyse glass fracture patterns and also his valuable comments and help during the course of the work. Special thanks are due to Professor Richard. C. Bradt, from Metallurgical and Materials Engineering Faculty, University of Alabama for his keen interest in the research work and also for kindly sending me some latest papers on glass fracture analysis.

I am much grateful and obliged to The Director, Royal Malaysia Police Forensic Laboratory, Batu 8 ½, Cheras, Selangor for his help and encouragement. I am greatly indebted to Mr. Mad Yussof bin Akop and Logistic (Firearm) Department, Malaysia Royal Police, Kuala Lumpur for his kind permission and assistance to conduct shooting experiments for the research work. Without his help and support, the research work carried out in the thesis would not be possible. I would like to thank Superintendent Muhammad Koey Abdullah for his help and advice.

I wish to extend my utmost gratitude and thankfulness to Inspector Rasyidi Harun, who has been much instrumental in the conduct of the experiments using different types of calibres and firearms. He had been quite spontaneous in providing all assistance during the bullet shooting experiments. His technical advice especially in the construction of firearm ransom rest used throughout the experiments has been of great help. My interactions with him during the ballistic tests have benefited me a lot. L/kpl/T Mr. Azlan Shamsul Kamar Abdul Rashid, Mr. Johari Rahidin, and Mr. Mohd Sharman Razaki deserve special mention for their help during shooting tests. Inspector Wan Zulizzi Wan Muda and SM Yaacob Abdullah from Firearms Unit Police Headquarters, Kelantan, are fondly remembered for their assistance.

I would like to thank Deputy Director of Development Department, Universiti Sains Malaysia, Kelantan for the help in the construction of the apparatus for ball dropping experiments. Not forgetting, I wish to thank Mr. Zahari Mamat from the same department, for assistance in performing ball dropping experiments.

I also wish to express my deep gratitude to Mr. Rose Samsuri Mamat, Mr. Rusli Mohammad and Mr. Muhammad Sham Mustapha, Photography Unit, Universiti Sains Malaysia, Kelantan for the photographic assistance in capturing images of glass fracture patterns. The many photographs that appear in the thesis attest to their valuable assistance. I would like to thank Biology Laboratory, Universiti Sains Malaysia, Penang for their help by conducting the scanning electron microscope.

I wish to thank Mr. Malek Riduan and Mr. Mohd Firdaus Emran for their valuable help in the collection of bullets from the bullet catch after penetration through glass. Not forgetting, all staff and students of Forensic Science Programme, School of Health Sciences, Universiti Sains Malaysia, Health Campus for their willingness in helping and guiding me throughout this study. To all my colleagues, Amy, Chang, Izzati, Rezza Petra, Siti Zulfarina and others, thank you for the comments, suggestions and support.

I wish to thank my parents, Mr. Syed Mohd Daud and Mrs. Zaharah Jasmin, and my siblings, who provided me continuous enriching love, support, encouragement and inspiration to pursue my study.

My profound thankfulness goes to Universiti Sains Malaysia for the financial assistance sanctioned under Fundamental Research Grant Scheme (203/PPSK/6171102) that enabled me to have successfully carrying out this research work.

# TABLE OF CONTENTS

	PAGE
<b>ACKNOWLEDGEMENTS.....</b>	<b>ii</b>
<b>TABLE OF CONTENTS.....</b>	<b>v</b>
<b>LIST OF TABLES .....</b>	<b>ix</b>
<b>LIST OF FIGURES .....</b>	<b>xii</b>
<b>LIST OF ABBREVIATION.....</b>	<b>xviii</b>
<b>ABSTRAK.....</b>	<b>xix</b>
<b>ABSTRACT .....</b>	<b>xxi</b>
<b>CHAPTER 1- INTRODUCTION .....</b>	<b>1</b>
1.0 Introduction.....	1
1.1 Scope and Objectives of Research.....	3
1.2 Research Outline.....	4
<b>CHAPTER 2- LITERATURE REVIEW .....</b>	<b>5</b>
2.1 Glass Properties .....	5
2.2 Glass Fracture Process .....	7
2.2.1 Low velocity impact fractures (quasi-static loading) .....	8
2.2.2 High velocity impact fractures (dynamic loading) .....	9
2.2.2 (a) Crater formation .....	10
2.2.2 (b) Fracture pattern.....	12
2.2.2 (c) Sequence of shots .....	15
2.3 Glass Fracture Surface Markings.....	17
2.3.1 Mirror .....	17
2.3.2 Mist.....	18
2.3.3 Rib marks.....	19
2.3.4 Hackle marks .....	21
2.4 Fractal Geometry .....	23
<b>CHAPTER 3- MATERIALS AND METHODS.....</b>	<b>24</b>
3.0 Introduction.....	24
3.1 Low Velocity Glass Target Impact experiments.....	25
3.2 Bullet Impact Experiments .....	27
3.2.1 Materials .....	27
3.2.1 (a) Window glass panes .....	27
3.2.1 (b) Firearms and ammunitions .....	28
3.2.1 (c) Impact test stand.....	33

3.2.1 (c) (i) Firearm rest .....	33
3.2.1 (c) (ii) Bullet velocity measurement.....	34
3.2.1 (c) (iii) Target glass stand.....	36
3.2.1 (c) (iv) Bullet catch.....	37
3.2.2 Experimental system.....	38
3.2.2 (a) Experimental apparatus .....	38
3.2.2 (b) Experimental designs .....	40
3.2.2 (c) Recovery of deformed bullets .....	45
3.2.2 (d) Transportation of broken glass panes for laboratory examination .....	45
3.3 Examination Procedure.....	46
3.3.1 Examination of glass fracture patterns .....	46
3.3.2 Microscopic examination of fracture surfaces.....	47
3.3.2 (a) Optical microscope.....	47
3.3.2 (b) Scanning electron microscope.....	48
3.3.2 (c) Measurements of bullet deformation.....	49
3.3.2 (d) Determination of fractal dimensions of fracture patterns.....	49
<b>CHAPTER 4- RESULTS.....</b>	<b>52</b>
4.1 General Physical Characteristics of Glass Fractured by Drop Ball Tests .....	52
4.1.1 Fracture patterns by varying speeds of the dropping ball.....	56
4.1.2 Fracture surface markings .....	59
4.2 General Physical Characteristics of Glass Fractured by Bullet Impacts.....	60
4.2.1 Glass fracture patterns .....	60
4.2.2 Fracture surface markings .....	63
4.2.2 (a) Rib marks .....	63
4.2.2 (b) Hackles.....	65
4.2.2 (c) Crack branching .....	68
4.2.2 (d) Repeating mirror, mist and hackle.....	71
4.3 Glass Fractured by Ammunitions of Different Types of Calibres .....	73
4.3.1 Calibre 7.65 mm FMJ.....	73
4.3.2 Calibre SME .38 in. Special (Revolver).....	79
4.3.2 (a) Fracture pattern glass by varying target glass thickness.....	85
4.3.3 Calibre 9 mm SME FMJ (pistol) .....	92
4.3.4 Calibre 9 mm Luger FMJ (SMG).....	97
4.3.4 (a) Fracture patterns caused by varying bullet speeds .....	101
4.3.4 (b) Fracture patterns caused by varying glass dimension .....	110
4.3.5 Calibre 9 mm Luger Flat Nose (pistol).....	113
4.3.6 Calibre 9 mm Luger Flat Nose (SMG).....	118
4.3.6 (a) Fracture patterns caused by varying glass dimension .....	123

4.3.7	Calibre 9 mm Luger Hollow Point (pistol).....	126
4.3.8	Calibre 9 mm Luger Hollow Point (SMG).....	131
4.3.9	Calibre 5.56 mm FMJ (Rifle) .....	136
4.3.9 (a)	Fracture patterns caused by varying bullet speeds .....	141
4.3.9 (b)	Fracture patterns caused by varying glass dimension .....	146
4.3.10	Calibre 5.56 mm FMJ (carbine) .....	149
4.3.10 (a)	Fracture patterns caused by varying bullet speeds .....	154
4.3.10 (b)	Fracture patterns caused by varying target glass thickness .....	163
4.3.11	Calibre 7.62 mm FMJ (Rifle) .....	169
4.3.11 (a)	Fracture patterns caused by varying glass dimension .....	174
4.4	Summary of characteristics of fracture patterns and cross sectional markings caused by different types of ammunition.....	177
4.4.1	Characteristics of fracture patterns.....	177
4.4.2	Characteristics of fracture surface (cross sectional) markings .....	184
<b>CHAPTER 5- DISCUSSIONS .....</b>		<b>190</b>
5.1	Low Level Velocity Impacts.....	190
5.2	Bullet Impacted Glass .....	190
5.2.1	Deflection of radial cracks.....	191
5.2.2	Repeating mirror, mist, hackle and crack branching zones .....	192
5.3	Characteristics of Glass Fractured by Different Types of Ammunition and Calibres .....	193
5.3.1	Bullet holes .....	193
5.3.2	Craters.....	194
5.3.3	Fracture patterns .....	195
5.3.3 (a)	Influence of nose shapes.....	195
5.3.3 (b)	Effects of bullet velocity .....	197
5.3.4	Fracture surface markings .....	199
5.3.4 (a)	Ribs.....	199
5.3.4 (b)	Hackles .....	200
5.3.5	Influence of the size and thickness of the target glass .....	201
5.3.5 (a)	Size of the target glass.....	201
5.3.5 (b)	Target glass thickness.....	204
5.3.6	Dependence on the energy absorbed by the target glass .....	204
5.4	Bullet Deformation .....	206
5.5	Relation between Striking Velocity/Energy and Remaining Velocity/Energy .....	207
5.6	Deviations from the Normal Crack Patterns .....	208
<b>CHAPTER 6- CONCLUSIONS.....</b>		<b>211</b>
6.1	Overview.....	211

6.2	Achievement of This Study .....	211
6.3	Limitations .....	213
6.4	Recommendations for Future Study .....	214
<b>REFERENCES .....</b>		<b>215</b>
<b>APPENDICES .....</b>		

## LIST OF TABLES

	<b>PAGE</b>
<b>Table 3.1:</b> Physical and mechanical properties of soda lime glass. ....	28
<b>Table 3.2:</b> Description of firearms and ammunitions used in this study.....	29
<b>Table 3.3:</b> Parameters tested in the glass shooting experiments.....	44
<b>Table 4.1:</b> Summary of fracture patterns of 2 mm thickness glass at various heights and speeds .....	58
<b>Table 4.2:</b> Percentage of two deformed bullets of 7.65 mm FMJ calibres shot from a Walther pistol.....	76
<b>Table 4.3:</b> Striking velocity, remaining velocity, striking and remaining momentum, initial energy, remaining energy, and loss for the broken glass panes caused by 7.65 mm FMJ calibres fired from Walther pistol. ....	77
<b>Table 4.4:</b> Bullet deformations of .38 in. Special calibre shot from revolver. Both bullets yielded similar deformation percentages which were compatible with the fracture patterns. ....	80
<b>Table 4.5:</b> Striking velocity, remaining velocity, striking momentum, remaining momentum, initial energy and remaining energy and their loss for the broken glass panes caused by .38 in. Special fired from revolver.....	83
<b>Table 4.6:</b> Features of glass by varying the glass thickness caused by .38 in. Special. ....	86
<b>Table 4.7:</b> Shows the striking, remaining velocity, velocity loss, momentum loss, kinetic energy loss for various glass thickness of .38 in. Special calibres.....	89
<b>Table 4.8:</b> Bullet deformation of .38 in. Special calibres shot from the revolver. Bullets deformation was compatible with the fracture patterns. ....	90
<b>Table 4.9:</b> Bullet deformation of 9 mm SME FMJ calibres .....	95
<b>Table 4.10:</b> Striking and remaining velocity, striking and remaining momentum, initial and remaining energy and their loss for the broken glass panes caused by 9 mm SME FMJ calibres fired from G-Lock pistol.....	95
<b>Table 4.11:</b> Bullet deformation of 9 mm Luger FMJ calibre fired from Bushmaster SMG. The bullet yielded more deformation than 9 mm Luger calibre fired from the pistol.....	99
<b>Table 4.12:</b> Striking and remaining velocity, initial and remaining momentum, initial and remaining energy, and their loss for broken glass panes caused by 9 mm Luger FMJ calibres fired from Bushmaster SMG. ....	99
<b>Table 4.13:</b> The features of glass fracture patterns by varying speed of the bullets of 9 mm Luger FMJ (SMG). ....	104
<b>Table 4.14:</b> Striking and remaining velocity, momentum, and energy and loss of velocity, momentum, and kinetic energy for all impact velocities .....	105
<b>Table 4.15:</b> Bullet deformations of 9 mm Luger fired from SMG by varying impact velocities. The value was arranged in the decreasing of kinetic energy loss. ....	108
<b>Table 4.16:</b> Bullet deformation of 9 mm Luger FMJ fired on a larger glass. Almost half of the bullet size was deformed (46.59 %). ....	110

<b>Table 4.17:</b>	Striking, remaining and loss of velocity, momentum and energy for larger glass panes caused by 9 mm Luger FMJ fired from SMG .....	112
<b>Table 4.18:</b>	Bullet deformations of 9 mm FMJ Flat nose calibre with similar percentages of deformation; hence created similar glass fracture patterns .....	116
<b>Table 4.19:</b>	Striking velocity and remaining velocity, initial and remaining momentum, initial energy and remaining energy and each loss for the broken glass panes caused by 9 mm Luger FMJ Flat nose calibres fired from G-Lock pistol.....	116
<b>Table 4.20:</b>	Bullet deformations of 9 mm Luger FMJ Flat nose calibre fired from SMG. The bullet yielded more deformation than those fired from the pistol (41.41%). .....	121
<b>Table 4.21:</b>	Striking and remaining for velocity, momentum and energy for all the broken glass panes caused by 9 mm Luger Flat nose calibres fired from Bushmaster SMG.....	121
<b>Table 4.22:</b>	Bullet deformations of 9 mm Luger Flat nose impacted on larger sized glass.....	123
<b>Table 4.23:</b>	Striking velocity along with remaining velocity, initial and remaining momentum, initial energy and remaining energy and loss of 9 mm Luger Flat nose impacted on larger glass. ....	125
<b>Table 4.24:</b>	Bullet deformations of 9 mm Luger FMJ Hollow point fired from pistol where bullet number two has higher percentage of deformation compared to number one due to higher kinetic energy loss. ....	129
<b>Table 4.25:</b>	Striking velocity, remaining velocity, initial energy and remaining energy for all the broken glass panes caused by 9 mm Luger FMJ Hollow point calibres fired from G-Lock pistol. ....	129
<b>Table 4.26:</b>	Percentages of bullet deformations of 9 mm Luger FMJ Hollow point bullets is shown. ....	134
<b>Table 4.27:</b>	Striking velocity, momentum, and energy, remaining velocity, momentum and energy and loss for all the broken glass panes caused by 9 mm Luger Hollow point calibres fired from Bushmaster SMG. ....	134
<b>Table 4.28:</b>	Bullet deformations of rifle ammunition .....	139
<b>Table 4.29:</b>	Striking velocity, momentum and energy, remaining velocity, momentum, and energy and loss for the broken glass panes caused by 5.56 mm FMJ fired from M16A Rifle. ....	139
<b>Table 4.30:</b>	Striking, remaining velocity, velocity loss, momentum loss and kinetic energy loss for all impact velocities. ....	144
<b>Table 4.31:</b>	Bullet deformations of 5.56mm fired from rifle on larger glass.....	148
<b>Table 4.32:</b>	Striking velocity, momentum and energy, remaining velocity, momentum, and energy and loss for larger dimensional glass caused by 5.56 mm FMJ fired from rifle.....	148
<b>Table 4.33:</b>	Shows the percentage of bullet deformations for both bullets caused by 5.56 mm FMJ discharged from carbine.....	152
<b>Table 4.34:</b>	Striking and remaining velocity, momentum and energy with their loss for all the broken glass panes caused by 5.56 mm FMJ fired from carbine. ....	152
<b>Table 4.35:</b>	Striking, remaining velocity, initial energy, remaining energy, velocity loss, momentum loss and kinetic energy loss for all impact	

	velocities.....	159
<b>Table 4.36:</b>	Bullet deformation of 5.56 mm discharged from carbine by varying the speed of bullets. ....	162
<b>Table 4.37:</b>	Striking, remaining velocity, velocity loss, momentum loss, kinetic energy loss and bullet deformations for all glass thickness.....	167
<b>Table 4.38:</b>	Bullet deformations of 5.56 mm FMJ by varying the glass thickness.....	168
<b>Table 4.39:</b>	Two deformed bullets of 7.62 mm calibre fired from M70 rifle. ....	172
<b>Table 4.40:</b>	Striking velocity, remaining velocity, striking and remaining momentum, initial energy and remaining energy and their loss for broken glass panes caused by 7.62 mm FMJ calibres fired from M70 rifle. ....	172
<b>Table 4.41:</b>	Bullet deformation was slightly more than bullet shot at smaller glass dimension, 300 x 300 x 5 mm <sup>3</sup> .....	176
<b>Table 4.42:</b>	Striking velocity, remaining velocity, striking and remaining momentum, initial energy and remaining energy and their loss for broken glass panes caused by 7.62 mm FMJ calibres fired from M70 rifle. ....	176
<b>Table 4.43(a):</b>	Details of measurements made on crater. ....	177
<b>Table 4.43(b):</b>	Radial, deflected radial and bifurcated fracture patterns caused by various types of ammunition. ....	179
<b>Table 4.44:</b>	Fracture patterns caused by different types of ammunition observed on 5 mm thick glass target.....	181
<b>Table 4.45:</b>	Cross section markings caused by different types of ammunition .....	184

## LIST OF FIGURES

		PAGE
<b>Figure 2.1</b>	Glass fracture patterns on a soda lime glass plate caused by dropping a steel ball of mass 95.3 g from 70.0 cm height at 0° angle of impact .....	8
<b>Figure 2.2</b>	A crater is seen on glass on the side opposite to the direction of application of force after penetration of a bullet.....	11
<b>Figure 2.3</b>	Fracture patterns caused by shots on 2 mm thickness of soda lime glass caused by .38 in. Special calibre.....	16
<b>Figure 2.4</b>	(a) Mirror, (b) Mist, (c) Hackle regions on the fracture surface on a 5 mm thick glass, 16 ×.....	18
<b>Figure 2.5(a)</b>	Curved rib marks on radial cracks on a broken glass caused by 7.65 mm FMJ calibres shot from Walther 7.65 mm pistol .....	20
<b>Figure 2.5(b)</b>	Rib marks on concentric cracks of a glass fracture caused by 7.65 mm FMJ calibre fired from Walther 7.65 mm pistol, 7.1 ×.....	20
<b>Figure 2.6(a)</b>	Hackle marks on a radial crack surface produced by low velocity impact (3.10 m/ s), 32 ×. Arrow shows direction of force.....	22
<b>Figure 2.6(b)</b>	Hackle marks on a radial fracture surface caused by high velocity bullet impact (200 m/ s), 32 ×. The arrow shows the direction of force.....	22
<b>Figure 3.1</b>	Apparatus for ball dropping experiments .....	25
<b>Figure 3.2</b>	Firearms and ammunitions used in this study.....	30
<b>Figure 3.3</b>	The gun is placed firmly in the ransom of the firearm rest.....	34
<b>Figure 3.4</b>	Bullet velocity measurement, chronograph placed on a stable table.....	35
<b>Figure 3.5</b>	Glass fixed in the target glass stand.....	36
<b>Figure 3.6</b>	Projectile catch filled with cotton wool to catch the projectile.....	37
<b>Figure 3.7(a)</b>	Experimental set up used in the study .....	39
<b>Figure 3.7(b)</b>	The shooter aims at the glass target.....	39
<b>Figure 3.8</b>	The various steps necessary in order to reduce the propellant powder from the cartridge are illustrated.....	42
<b>Figure 3.9</b>	Leica MZ16 Stereomicroscope Research Grade attached with LAS software .....	48
<b>Figure 3.10(a)</b>	Two typical glass fracture patterns, 1 and 2 caused by .38 in. Special on 5 mm thick glass .....	51
<b>Figure 3.10(b)</b>	The fractal dimension was calculated to be respectively 1.386 and 1.388 .....	51
<b>Figure 4.1</b>	Crack patterns from dropping a ball (95.3 g) on 3 mm thickness glass from (a) 60.0 cm and (b) 65.5 cm height. Smooth and straight radial cracks and regularly formed concentric cracks around the point of impact are noticed.....	53
<b>Figure 4.2(a)</b>	Radial fracture surface of 3 mm thickness glass caused by dropping a ball of mass 95.3 g from 80.0 cm height. ....	54
<b>Figure 4.2(b)</b>	3 mm thickness glass was impacted by dropping a ball 95.3 g from 70.0 cm height The hackles along the edge of a radial fracture surface	

	are seen, 32 ×.....	54
<b>Figure 4.3</b>	SEM images of hackles shown in Fig. 4.2 (b) at different scale levels: (a) 100 ×, (b) 500 ×.....	55
<b>Figure 4.4</b>	The fracture patterns caused by dropping ball experiments, 95.3 g from various heights (h) on 2 mm thickness glass .....	57
<b>Figure 4.5</b>	Hackles on radial fracture surfaces of 2 mm thickness glass caused by dropping a ball from various heights and speeds, 115 × .....	59
<b>Figure 4.6</b>	(a) Crack patterns from 7.65 mm FMJ caliber and (b) 9 mm Luger FMJ calibre bullets fired respectively from Walther pistol and Bushmaster SMG at 5 mm thick glass.....	61
<b>Figure 4.7(a)</b>	Reversible ribs on the cross sections of radial fractures caused by 7.65 mm FMJ calibre (left) and .38 in. Special calibre (right), 7.1 ×.....	64
<b>Figure 4.7(b)</b>	Cross sections of deflected radial cracks caused by 7.65 mm FMJ calibre (left) and pistol 9mm Luger FMJ calibre (right), 7.1 × .....	64
<b>Figure 4.8</b>	SEM micrographs: a) Shows steps and welts on the fracture surface of deflected radial crack caused by 9 mm Flat Nose calibre shot from SMG, 40 × (b) Shows the details of image, 100 × (c) Viewed at higher magnification 500 ×, finer marks are seen .....	66
<b>Figure 4.9</b>	The presence of shear hackles in the end of crack caused by 5.56 mm FMJ calibre shot from M16A rifle.....	67
<b>Figure 4.10</b>	Mirror (a), mist (b), hackle (c), and crack branching (d) regions on fracture surface of a 5 mm thickness glass caused by: (a) 9 mm Luger FMJ shot from G-lock pistol, (b) 9 mm Flat nose shot by Bushmaster 9 mm SMG, 16 × .....	69
<b>Figure 4.11</b>	SEM images of the cross section caused by 5.56 mm FMJ calibre fired from carbine showing the transition of mirror to crack branching: (a) 35 ×, (b) 250 × and (c) 1000 × .....	70
<b>Figure 4.12</b>	Multiples of mirror, mist, hackles and crack branching regions on the radial fracture surfaces on the broken glass panes caused by 5.56 mm FMJ calibre shot from carbine, 7.1 ×.....	71
<b>Figure 4.13</b>	Anomalous fracture patterns on the radial fracture surfaces on the broken glass panes caused by 9 mm flat nose fired from SMG, 7.1 × .....	72
<b>Figure 4.14</b>	Two glass fracture patterns (a) and (b) caused by 7.65 mm FMJ calibre shot from a Walther 7.65 mm pistol at 5 mm thickness glass (aluminum frame).....	74
<b>Figure 4.15</b>	(a) Close up photographs of the crater areas shown in Fig. 4.14 (b) Two deformed bullets of 7.65 mm FMJ calibre with metal jackets.....	75
<b>Figure 4.16</b>	(a) Remaining velocity after target penetration as a function of striking velocity (b) Remaining energy after target penetration as a function of initial energy for broken glass panes caused by 7.65 mm FMJ calibres fired from Walther pistol .....	78
<b>Figure 4.17</b>	Two fractures patterns (a) and (b) caused by .38 in. Special fired from S&W revolver on 5mm thick glass.....	81
<b>Figure 4.18</b>	(a) Close up appearance of the crater areas of as shown in fig. 4.17 where large crater dimensions were observed (b) Two deformed bullets of .38 in. Special .....	82
<b>Figure 4.19</b>	(a) Remaining velocity after target penetration as a function of striking velocity (b) Remaining energy after target penetration as a	

	function of initial energy for broken glass panes caused by .38 in. Special fired from revolver.....	84
<b>Figure 4.20</b>	Evolution of glass fracture patterns with thickness of glass panes. .38 in. Special calibres fired from revolver .....	87
<b>Figure 4.21</b>	Close up of the crater area shown in Fig. 4.20 .....	88
<b>Figure 4.22</b>	Bullet deformations of .38 in. special after penetration of different glass thickness .....	90
<b>Figure 4.23</b>	Relationship between bullet deformations and kinetic energy loss .....	91
<b>Figure 4.24</b>	Relationship between fractal dimension and thickness of glass .....	91
<b>Figure 4.25</b>	Fracture patterns (a) and (b) on 5 mm thick glass caused by 9 mm SME FMJ fired from G- Lock pistol l.....	93
<b>Figure 4.26</b>	(a) Close up of the crater areas shown in Fig. 4.25 (b) Deformed bullets of 9 mm SME FMJ calibres .....	94
<b>Figure 4.27</b>	(a) Remaining velocity after target penetration as a function of striking velocity (b) Remaining energy after target penetration as a function of initial energy for broken glass panes caused by 9 mm SME FMJ calibres shot from G-Lock pistol.....	96
<b>Figure 4.28</b>	(a) Glass fracture patterns caused by 9 mm Luger FMJ calibre shot from SMG on 5mm thick glass (b) Close up of the crater areas of glass panes (c) The deformed bullet 9 mm Luger FMJ .....	98
<b>Figure 4.29</b>	(a) Remaining velocity after target penetration as a function of striking velocity (b) Remaining energy after target penetration as a function of initial energy for broken glass panes caused by 9 mm Luger FMJ calibres shot from Bushmaster SMG .....	100
<b>Figure 4.30</b>	Broken glass panes caused by 9 mm Luger calibres fired from SMG at all impact velocities ( $V_s$ ).....	102
<b>Figure 4.31</b>	Close up of the crater areas shown in Fig. 4.30.....	103
<b>Figure 4.32</b>	(a) Remaining velocity after target penetration as a function of striking velocity (b) Remaining energy after target penetration as a function of initial energy for broken glass panes caused by 9 mm Luger FMJ calibres shot from Bushmaster SMG .....	106
<b>Figure 4.33</b>	Bullet deformations of 9 mm Luger FMJ by varying the speed of bullets .....	107
<b>Figure 4.34</b>	Percentage of bullet deformation against kinetic energy loss of 9 mm FMJ calibres .....	109
<b>Figure 4.35</b>	Fractal dimension, FD plotted against kinetic energy loss .....	109
<b>Figure 4.36</b>	(a) Larger glass fracture patterns, 45 cm x 45 cm caused by 9 mm Luger FMJ calibre fired from SMG (b) Close up of the crater area (c) Almost half of the length of the bullet was deformed.....	111
<b>Figure 4.37</b>	Glass fracture patterns (a) and (b) caused by 9 mm FMJ Flat nose calibre fired from pistol at 5 mm thick glass .....	114
<b>Figure 4.38</b>	(a) Close up appearance of the crater areas shown in Fig. 4.37 (b) Two similar bullet deformations of 9 mm FMJ Flat nose bullets .....	115
<b>Figure 4.39</b>	(a) Remaining velocity after target penetration as a function of striking velocity (b) Remaining energy after target penetration as a function of initial energy for broken glass panes caused by 9 mm Luger FMJ Flat nose calibres fired from a G-Lock pistol .....	117

<b>Figure 4.40</b>	Two glass fracture patterns (a) and (b) caused by 9 mm Luger FMJ Flat nose calibre shot from SMG at 5 mm thick glass.....	119
<b>Figure 4.41</b>	(a) Glass fracture patterns produced deflected radial cracks near the crater area (b) Bullet deformation on the right produced greater deformation, 42.07% and 47.42% respectively .....	120
<b>Figure 4.42</b>	(a) Remaining velocity after target penetration as a function of striking velocity (b) Remaining energy after target penetration as a function of initial energy for broken glass panes caused by 9 mm Luger FMJ Flat nose calibres shot from Bushmaster SMG.....	122
<b>Figure 4.43</b>	a) Glass fracture patterns on glass 450 x 450 x 5 mm <sup>3</sup> caused by 9 mm Luger FMJ Flat nose calibre fired from SMG (b) Close up on crater area as shown by top picture.....	124
<b>Figure 4.44</b>	Two glass fracture patterns (a) and (b) caused by 9 mm Luger FMJ Hollow point pistol bullets at 5 mm thick glass .....	127
<b>Figure 4.45</b>	(a) Crater appearances of glass fracture patterns as shown in Fig. 4.44 (b) Bullet on the right has greater deformation, 34.84% hence has created a greater damage to crater area compared to the bullet on the left which has 15.82% of deformation.....	128
<b>Figure 4.46</b>	(a) Remaining velocity after target penetration as a function of striking velocity (b) Remaining energy after target penetration as a function of initial energy for broken glass panes caused by 9 mm Luger FMJ Hollow point calibres shot from G-Lock pistol .....	130
<b>Figure 4.47</b>	Two glass fracture patterns (a) and (b) caused by 9 mm Luger FMJ Hollow point fired from SMG at 5 mm thick glass .....	132
<b>Figure 4.48</b>	(a) Close up appearances of crater area shown in Fig. 4.47 (b) Similar bullet deformations were yielded by both bullets and both have jackets separated.....	133
<b>Figure 4.49</b>	(a) Remaining velocity after target penetration as a function of striking velocity (b) Remaining energy after target penetration as a function of initial energy for broken glass panes caused by 9 mm Luger FMJ Hollow point calibres shot from Bushmaster SMG.....	135
<b>Figure 4.50</b>	Two glass fracture patterns (a) and (b) caused by 5.56 mm FMJ calibers fired from M16A rifle on 5 mm thick glass .....	137
<b>Figure 4.51</b>	(a) Crater area on the left yielded more dominant wing cracks and deflected radial cracks compared to the crater area on the right (b) Bullet on the left has more flattening on the tip and hence created more damage to the crater area.....	138
<b>Figure 4.52</b>	(a) Remaining velocity after target penetration as a function of striking velocity (b) Remaining energy after target penetration as a function of initial energy for broken glass panes caused by 5.56 mm FMJ calibres shot from M16A Rifle.....	140
<b>Figure 4.53</b>	Broken glass panes caused by 5.56 mm calibers fired from M16A rifle with varying projectile velocity ( $V_s$ ).....	142
<b>Figure 4.54</b>	Close up of the crater area of glass panes seen in Fig. 4.53 .....	143
<b>Figure 4.55</b>	(a) Remaining velocity after target penetration as a function of striking velocity (b) Remaining energy after target penetration as a function of initial energy for broken glass panes caused by 5.56 mm FMJ fired from M16A rifle .....	145

<b>Figure 4.56</b>	Fractal dimension, FD plotted against kinetic energy loss .....	146
<b>Figure 4.57</b>	(a) Larger glass fracture patterns, 45 cm x 45 cm caused by 5.56 mm FMJ calibre fired from M16A rifle (b) Close up on crater area (c) The deformed bullet .....	147
<b>Figure 4.58</b>	Two glass fracture patterns (a) and (b) caused by 5.56 mm FMJ ammunition fired from carbine on 5mm thick glass.....	150
<b>Figure 4.59</b>	(a) Close up of the crater area as shown in Fig. 4.58 (b) Similar bullet deformations were yielded by both bullets .....	151
<b>Figure 4.60</b>	(a) Remaining velocity after target penetration as a function of striking velocity (b) Remaining energy after target penetration as a function of initial energy for broken glass panes caused by 5.56 mm FMJ fired from Carbine.....	153
<b>Figure 4.61</b>	Crack patterns of glass panes caused by 5.56 mm calibres fired from carbine with varying projectile velocity (kinetic energy).....	155
<b>Figure 4.62</b>	Close up of the crater area of glass as shown in Fig. 4.61 .....	157
<b>Figure 4.63</b>	(a) Remaining velocity after target penetration as a function of striking velocity (b) Remaining energy after target penetration as a function of initial energy for broken glass panes caused by 5.56 mm FMJ fired from Carbine.....	160
<b>Figure 4.64</b>	Fractal dimension, FD for 5.56 mm fired from Carbine for different energy losses.....	161
<b>Figure 4.65</b>	Bullet deformation of 5.56 mm calibre (carbine) is arranged according to decreasing of kinetic energy loss (from left) .....	162
<b>Figure 4.66</b>	Bullet deformations plotted against kinetic energy loss .....	163
<b>Figure 4.67</b>	Glass fracture patterns at different glass thickness from 2 mm to 10 mm caused by 5.56 mm calibre shot from carbine.....	165
<b>Figure 4.68</b>	Close up of the crater areas of different thickness of glass panes as shown in Fig. 4.67 .....	166
<b>Figure 4.69</b>	Bullet deformations plotted against kinetic energy loss .....	168
<b>Figure 4.70</b>	Glass fracture patterns caused by 7.62 mm fired from M70 rifle.....	170
<b>Figure 4.71</b>	(a) Close up of the crater area as shown in Fig. 4.70 (b) Similar bullet deformations were yielded by both bullets .....	171
<b>Figure 4.72</b>	(a) Remaining velocity against striking velocity (b) Remaining energy plotted against striking energy for 7.62 mm calibre .....	173
<b>Figure 4.73</b>	(a) Glass fracture patterns on 450 x 450 x 5mm <sup>3</sup> caused by 7.62 mm FMJ calibre fired from M70 rifle (b) Close up of the crater area (c) The deformed bullet.....	175
<b>Figure 4.74</b>	Hackles here are long and fine and closely spaced with one another, 32 ×.....	187
<b>Figure 4.75</b>	Hackles here are long and coarse and closely spaced to one another, 32 ×.....	188
<b>Figure 4.76</b>	SEM images of hackles on deflected radial cracks caused by different calibres, 100 × (a) 5.56 mm calibres (carbine) were fine (b) 9 mm Flat Nose calibres (SMG) were coarse (c).38 in. Special calibres were coarse.....	189
<b>Figure 5.1</b>	Two shots (1) and (2) on the same glass pane which were sequentially	

	produced .....	203
<b>Figure 5.2</b>	(a) Glass fracture pattern caused by 9 mm flat nose calibre fired from G-Lock pistol (b) Close up of the crater area of the pattern (c) The bullet deformation was greater, 48.1% compared to the typical bullet deformation of 9 mm flat nose calibre.....	209
<b>Figure 5.3</b>	(a) Glass fracture pattern caused by 9 mm FMJ discharged from the G- Lock pistol (b) Close up of the crater area as shown above (c) Greater deformation, 48.27% was yielded by this calibre .....	210

## LIST OF ABBREVIATION

Au-Pd	Gold- palladium
CaO	Calcium Oxide
cm	Centimeter
D	Fractal dimension
D <sub>B</sub>	Box counting method
FMJ	Fully metal jacketed
g	Gramme
gr	Grain
In	Inch
J	Joule
mg	Milligramme
mm	Millimeter
MV	Momentum
m/s	Meter per second
Na <sub>2</sub> CO <sub>3</sub>	Sodium Carbonate
N s	Newton. Second
SiO <sub>2</sub>	Silicon dioxide
SMG	Sub machine gun

# **FENOMENA KERETAKAN DALAM KACA SODA KAPUR SILIKA DISEBABKAN OLEH KESAN PELURU**

## **ABSTRAK**

Satu siri kajian eksperimen di bawah keadaan terkawal telah dijalankan untuk menyiasat corak keretakan yang dihasilkan dalam bebanan statik (eksperimen menjatuhkan bola) dan juga kesan-kesan peluru daripada kaliber dan bentuk muncung yang berbeza, ditembak dengan senjata berbeza, ke atas kaca silika soda kapur yang mempunyai dimensi yang dan ketebalan berbeza. Keputusan yang diperolehi dalam ujikaji pembebanan statik mengesahkan penemuan awal yang dilaporkan dalam literatur. Semua peluru yang digunakan untuk ujikaji keretakan kaca yang dicetuskan oleh peluru, merupakan peluru bersalut logam penuh kecuali bagi peluru khas.38 inci yang berplumbum. Bentuk muncung berbeza termasuk bulat, rata dan titik berongga. Halaju peluru berubah-ubah dari 220 m/s kepada 1020 m/s. Dua kronograf, satu diletakkan di hadapan sasaran kaca dan satu lagi di belakangnya, mengukur halaju hentaman dan halaju baki peluru. Selepas peluru menembusi kaca, ia ditangkap dengan penangkap peluru. Kajian untuk mengenalpasti ciri-ciri dan penanda permukaan dijalankan pada corak keretakan yang terhasil. Sebahagian daripadanya juga dianalisis secara kuantitatif dengan menggunakan konsep dimensi fraktal yang mengukur kerumitan corak tidak teratur. Pemerhatian menunjukkan terdapat perbezaan yang besar dalam kelakuan peluru untuk menghasilkan corak keretakan pada kaca. Corak ini jauh berbeza berbanding dengan corak yang dihasilkan semasa ujian muatan statik. Setiap peluru daripada jenis dan kaliber tertentu menghasilkan corak yang unik yang dapat dikenalpasti. Peluru berkaliber yang sama (9mm muncung bulat dan muncung rata dan 5.56 mm kaliber rifel) dilepaskan dari dua senjata berbeza (pistol dan submesin-gan berkaliber 9 mm /dan rifel dan Carbine

berkaliber 5.56 mm) menghasilkan corak yang boleh dibezakan mengikut jenis pistol. Kecacatan pada peluru yang disebabkan oleh pengembangan dan hujung peluru yang mericih telah menunjukkan bahawa peluru adalah bersifat mulur pada halaju yang tinggi. Peratusan perubahan bentuk peluru menunjukkan hubungan linear kepada kerumitan akibat daripada corak keretakan: lebih besar peratusan lebih rumit corak yang terbentuk. Kehilangan halaju kaliber tertentu untuk ketebalan kaca hampir sama tanpa mengira halaju hentaman. Secara signifikannya dimensi fraktal corak berbeza secara linear dengan tenaga kinetik yang hilang kepada kaca semasa pemebusan peluru. Kajian mendapati dimensi kaca mempengaruhi corak keretakan. Kaca berdimensi besar mempunyai corak keretakan yang lebih kecil dan ciri-cirinya terbatas kepada kawasan yang dekat dengan lubang dan kawahnya. Sebaliknya, kaca berdimensi kecil merebak corak keretakan keseluruhan kaca. Ia boleh difahami secara kualitatif. Corak gelombang yang dihasilkan oleh impak peluru, yang mana bertanggungjawab untuk corak keretakan, dipengaruhi oleh keadaan sempadan pada bingkai kaca. Keadaan sempadan ini nyata mempengaruhi kesan kepada penyebaran gelombang dan mewujudkan lebih banyak apabila sempadan hampir ketahap impak peluru berbanding apabila ia jauh daripadanya. Kajian kuantitatif tentang pengaruh dimensi kaca ke atas corak keretakan harus dilakukan. Data dan analisis yang disertakan dalam tesis menunjukkan bahawa data dan analisis tersebut boleh digunakan dalam pembinaan semula tempat kejadian jenayah yang melibatkan insiden sebenar menembak termasuk di mana peluru telah melalui sasaran kaca terdekat. Soda kaca silika kapur didapati digunakan secara meluas untuk tingkap bangunan dan ia juga merupakan komponen penting dalam kaca berlapis dan kalis peluru. Kajian semasa, didapati, juga akan membantu para saintis bahan untuk memahami tingkah laku jenis kaca akibat impak peluru berhalaju tinggi supaya pembinaan kaca kalis peluru yang lebih baik dapat dihasilkan.

# **FRACTURE PHENOMENA IN SODA LIME SILICA GLASS CAUSED BY BULLET IMPACTS**

## **ABSTRACT**

A series of studies was performed under controlled experimental conditions to investigate the fracture patterns produced in static loading (ball dropping experiments) and also the impacts of bullets of different calibres and nose shapes, fired from different weapons, onto soda lime silica glass of different dimensions and thicknesses. The results obtained in static loading experiments confirmed the earlier findings reported in the literature. In the bullet induced glass fracture experiments, all the bullets were fully metal jacketed except .38 in. Special ones that had exposed lead. Nose types varied from round nose and flat nose to hollow point. The velocity of the bullets varied from 220 to 1020 m/s. Two chronographs, one placed in front of the glass target and the other immediately behind it, measured the striking and remaining velocities of the bullets. The bullets after penetration of the glass were recovered using a bullet catch. The resulting crack patterns on glass were studied for their characteristics and surface markings. Some of them were also analysed quantitatively using the concept of fractal dimension that measured the complexity of irregular patterns. Observations revealed substantial differences in the behaviour of the bullets to produce fracture patterns in the glass. These patterns were much different from those produced during static loading tests. Each bullet of a specific calibre and type produced a unique pattern by which it can be identified. Further, the same calibre bullets (9 mm round nose and flat nose, and 5.56 mm rifle calibre) discharged from two different weapons (pistol and sub machine gun for 9 mm calibre/ and rifle and Carbine for 5.56 mm calibre) produced distinguishable patterns according to each weapon. The bullets deformed by mushrooming and shearing of its

tip confirming the ductile nature of the projectiles at high velocities. The percentage of bullet deformation showed linear relationship to the complexity of the resulting fracture pattern: the greater the percentage the more complicated the patterns that were formed. The velocity loss for a specific calibre for a given thickness of glass was almost same irrespective of the striking velocity. Significantly, the fractal dimensions of the patterns varied linearly with the kinetic energy lost to glass during the penetration of the bullet. It was found that the dimension of the glass target had an influence in the fracture patterns caused. The larger dimensional glass had less cracking patterns and the characteristics were confined mostly to the regions close to the hole and the crater. The smaller dimensional glass had the patterns spread throughout the glass. This can be understood qualitatively. The waves that were setup in the glass by the impact of the bullet, responsible for the fracture pattern, were influenced by the boundary conditions obtained at the glass frame. These boundary conditions obviously affected the propagation of the waves created more when the boundary is near to the point of bullet impact than when it is far away. A quantitative study of the influence of glass dimensions on the fracture patterns should be worthwhile. The data and analysis presented in the thesis demonstrated that they can be used in real crime scene reconstructions involving shooting incidents including those in which bullets have passed through intermediate glass targets. Soda lime silica glass finds extensive use in the windows of buildings and it is also an important glass component in laminated and bullet proof glass. The current study might also help the material scientists to understand better the behaviour of this type of glass subjected to high velocity bullet impacts so that better bullet proof glass constructions could be conceived.

## CHAPTER 1

### INTRODUCTION

#### 1.0 Introduction

Forensic science is the application of a broad spectrum of sciences to answer questions of interest to the legal system (Seddon and Fass, 2009; Jackson and Jackson, 2008; Saferstein, 2006; Horswell, 2004). One of the major areas of forensic science is the analysis of fractures in glass. Forensic scientists are often being asked to examine broken glass to reconstruct events surrounding a crime or to associate a person or an object with the scene of the crime or a victim (Almirall *et al.*, 2000). Glass has been a crucial piece of information encountered in day to day life in burglary, arson, assault with a firearm, and motor vehicle accident (Waghmare *et al.*, 2003; O'Hara and O'Hara, 1994). Hence it is one of the most frequently investigated evidence materials by forensic scientists.

Characterisation of fracture phenomena in glass has been a subject of considerable forensic concern for several decades. The behaviour of glass under impact has been studied by material scientists for failure analysis (Bradt *et al.*, 2003; Bouzid *et al.*, 2001; West *et al.*, 1999; Miyamoto and Murakami, 1998; Ball, 1997). The use of glass in transparent armours against ballistic threats requires analysis of its response to impact (Grujicic *et al.*, 2009; Brajer *et al.*, 2003).

The study and analysis of glass impacts and the resulting crack patterns provide knowledge that can lead to improved design for increase in the impact resistance. These studies also benefit forensic investigations of impact failures, particularly the need to establish the cause of failure following an accident that involves a glass impact fracture (Bradt *et al.*, 2003). The manner in which a sheet of glass cracks under the stress of impulsive forces during bullet impacts is known to have characteristics quite different from those involving the impact of objects at relatively low velocities (Thornton and Cashman, 1986).

Broken glass exhibits unique fracture patterns and the surface markings depend upon the nature of the impact. The examination and interpretation of glass fractures provide a wealth of interpretable information in criminal investigation. The fracture patterns generally provide information regarding the point and angle of impact, direction of force and sequence of firing (Haag, 2004; McJunkins and Thornton, 1973; Smith, 1970).

Over the years, a number of papers have been published on various aspects of glass fracture (Bradt *et al.*, 2003; Shinkai, 1994). The process of glass fracture and the fracture surface characteristics have been studied by earlier researchers (Hull, 1999; Kepple and Wasyluk, 1994). Although there have been considerable efforts to study the fracture patterns of glass under impact, the relationships existing among the fracture patterns and the projectile impact factors such as bullet type and calibre, its shape and velocity are not well documented.

## **1.1 Scope and Objectives of Research**

The scope of the study was limited to patterns produced by orthogonal impacts. Experiments were designed meticulously under controlled impact conditions to characterise the response of glass to bullet impacts. For the purpose of this research, soda lime silica glasses were impacted with different calibres and types of bullets by varying the glass target thickness and also the nose geometry of the bullets. Tests were also conducted at various striking velocities by varying the quantity of smokeless propellant used. The dependence of glass fracture patterns and surface markings on various bullet parameters was established. The results were also compared with those of low velocity impacts (drop ball experiments).

The general objective was to confirm that bullets of different calibers and types cause unique fracture patterns and surface markings by which they could be distinguished. The specific objectives are:

- (1) to establish the nature of relationship between the fracture characteristics and projectile parameters using fractal geometry,
- (2) to determine the relationships between fractal dimensions and energy of bullets

## **1.2 Research Outline**

Review of related literature is presented in Chapter 2. The apparatus and experimental designs are described in Chapter 3. The various glass fracture characteristics arising from variations in calibre, bullet velocity and bullet and gun type, thickness and dimension of target glass are described in Chapter 4. Chapter 5 discusses the results of the fracture phenomena, in terms of bullet nose geometry, kinetic energy loss and fractal dimension of fracture patterns. Finally Chapter 6 gives a summary of the results together with recommendations for future research.

## CHAPTER 2

### LITERATURE REVIEW

#### 2.1 Glass Properties

Glass is an inorganic product of fusion which has been cooled to a rigid condition without crystallisation (Almirall *et al.*, 2000). The common glass used to manufacture windows for buildings, automobiles and containers is known as soda lime silica glass. The major composition of this glass is sand ( $\text{SiO}_2$ , 63 to 74%), soda ash ( $\text{Na}_2\text{CO}_3$ , 12 to 16%), limestone ( $\text{CaO}$ , 7 to 14%) and miscellaneous other oxides. Sand is of high quality and requires high temperature to melt, thus soda ash are added to lower the melting point (Almirall *et al.*, 2000). Limestone is added to decrease the solubility of the glass. As finishing, other oxides are added depending on the use of the product (Haag, 2004).

The common properties of glass are isotropic, elastic, hard, non- conductors of electricity and chemically stable (Wünsche *et al.*, 1997; Brechet and Neda, 1995). The isotropic characteristic is due to the random ordering of the atoms in the matrix structure, while elasticity of glass is limited primarily to short duration loads (McJunkins and Thornton, 1973).

There are three forms of glass that are commonly encountered in shooting incidents (Haag, 2004). The name flat glass has been used for the basic form of soda lime silica glass. The vast majority of flat glass used in the industry is float glass. The molten glass will undergo float process with incorporation of a liquid tin where the glass floats over the metal. This float process will lead to a smooth and flat surface of glass

(Houck and Siegel, 2010; Almirall *et al.*, 2000). The common thickness of this glass is between 2 mm and 12 mm. Sheets of thin glass would typically be found in small picture frames whereas the thicker forms are used in common windows in homes and commercial buildings (Haag, 2004).

Two or more sheets of the soda lime float glass are joined together with one or more viscous plastic layers between them to form a sort of sandwich. This is so-called laminated glass and is the standard for windshields in many automobiles. These panels of glass with thin polyvinyl plastic layer between them are typically moulded to have curvature due to their use in modern automobiles (Hueske, 2005; Haag, 2004).

A third form of glass is called tempered glass or double strength glass. It is used in many applications such as automobile windows, also in a redundant number of applications such as commercial store, doorway windows and glass enclosed shower stalls. It is much stronger than for the same thickness of plate glass. However, when it fails, it instantaneously breaks into many small pieces that are generally cubic or rectangular in shape. This is called dicing and it is a desirable feature from an enhanced safety standpoint because of its greater resistance to breakage and reduced likelihood of causing serious injuries when it is broken (Siegel, 2007; Haag, 2004).

Bullet resistant glass or simply impact resistant glass is a glass/polymer composition of multilayer laminate design. The exterior layers are usually soda-lime-silicate float glass to resist scratching and maintain transparency. A polymer, often polycarbonate, is sandwiched between the outer glass layers (Yoshimura and Morrone, 2006). The utilisation of impact resistant glass is continually increasing in applications that range from wind damage prevention during storms to that of bullet proofing applications in automobile windows.

## 2.2 Glass Fracture Process

Typically, a pane of glass will break in a specific way when a force of a blow or a projectile is applied. The fracture patterns that show on a broken glass are unique (Koons *et al.*, 2002). These fracture features reflect the nature of the glass, the direction of travel and the cause of failure (Rhodes *et al.*, 1975). Types of glass encountered in crime scene investigation include normal window glass, safety glass, tempered glass and bullet resistant glass. Each type of glass shows a different behaviour at the impact of a projectile (De Kinder *et al.*, 2002).

Glass fractures are divided into two categories which is low velocity impact fractures (quasi-static loading) and high velocity impact fractures (dynamic loading). Quasi static loading is the type of stress where the application of force onto the glass is slow about a few hundredths of a second or a less whereas dynamic loading is the type of stress where the application of force onto the glass is very rapid, that is for about a few microseconds (Thornton and Cashman, 1986).

## 2.2.1 Low velocity impact fractures (quasi-static loading)

Figure 2.1 shows the glass fracture patterns on a piece of soda lime glass caused by low velocity impact. In low velocity impact fractures, the application of force onto the glass is relatively slow. When a force is applied to a glass, the glass bends in the direction in which it was applied. Tensile stress will be created on the opposite side of force and compressive force on the side of force. The glass will fail under the tensile stress since glass is weaker under tensile than compression with cracks being initiated on the opposite side of force (Kurkjian, 2002). These cracks are rapidly propagated and they radiate outwards and away from the point of impact. These cracks are known as radial cracks (Thornton and Cashman, 1986).

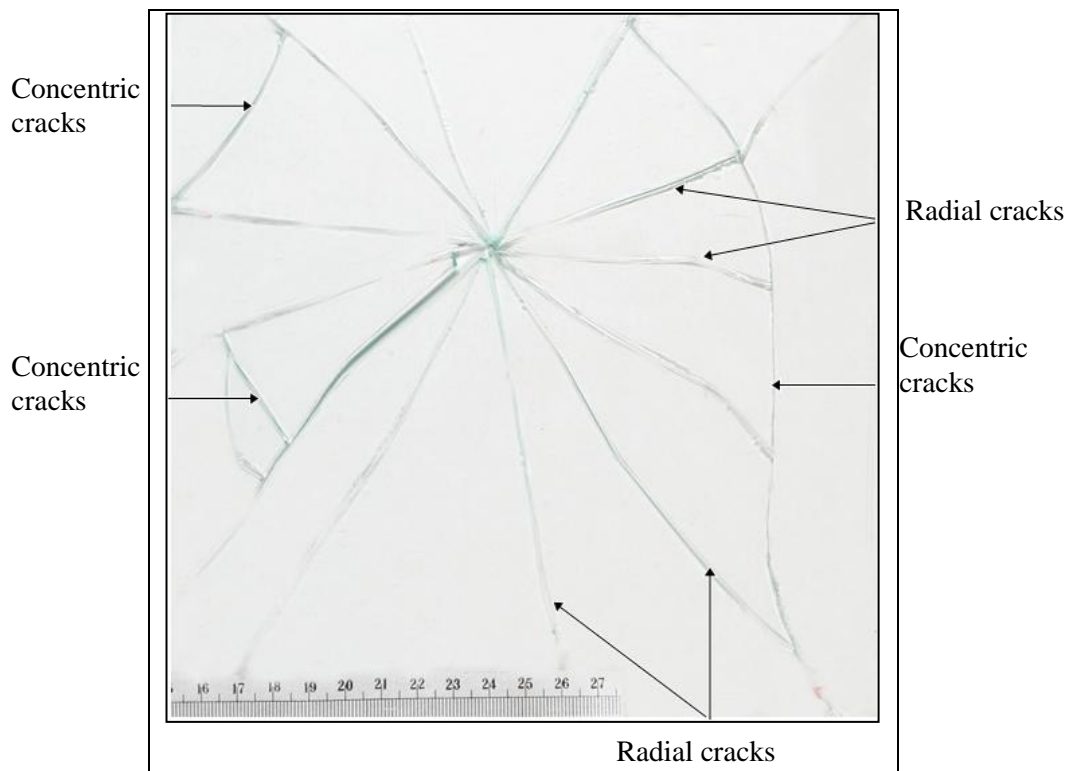


**Figure 2.1:** Glass fracture patterns on a soda lime glass plate caused by dropping a steel ball of mass 95.3 g from 70.0 cm height at 0° angle of impact.

The hole must be created before the radial cracks, as the radial cracks originate from the point of impact (Astrom and Timonen, 1997). After the radial cracks are formed, the fracture may be completed at this point. However, in some circumstances, there is still an accumulation of stress that has yet to be relieved. In such cases, the continued stress will place tension on the front surface of the glass. The glass is then pushed toward the front surface with fracture starting on the front side and extending between two adjacent radial fractures. These fractures are formed in the form of circular arcs around the point of impact, and are therefore termed concentric cracks (Matwejeff, 1931). Usually, concentric cracks are formed when a pane of glass is held firmly on all sides at the moment of the application of force (Koons *et al.*, 2002).

### **2.2.2 High velocity impact fractures (dynamic loading)**

In high velocity impact fractures, dynamic loading mechanism is involved. When a high velocity projectile strikes a pane of glass, longitudinal mechanical waves are produced. These waves begin at the point of impact and radiate outward in a series of spherical wave fronts. The wave fronts travel through the glass at higher velocity than the projectile itself, approximately 5000 m/s at a time (Thornton and Cashman, 1986).

When the wave front, or known as compression wave, is produced at the opposite side of the glass, it is reflected and it becomes a tension wave. When the tension wave strikes the front side, it will be reflected again as a compression wave and again reflected as a tension wave toward opposite side. These phenomena of reflection of strain waves will induce the interference of tension waves. At this moment, the amplitude of waves and tensile strength will be increased. As a result, the glass will be broken (Tryhorn, 1939).

The earliest discussion regarding the bullet fractures was published by Hans Gross (1906) as an aid in the resolution of forensic issues. Gross reported that window fractures impacted by high velocity projectiles were dependent on the velocity and angle of impact. He noted that if the velocity was sufficiently high, the window would display a round, clean hole and bevelled out toward the exit side. Gross claimed that the bevelling which was in shell shaped fractures was present on the reverse side of the bullet hole (cited by McJunkins and Thornton, 1973).

The shell shaped fractures present at the exit side resulting from very high tensile stresses is called crater which is one of the fracture characteristics of bullet impacts. Other than crater, radial and concentric cracks are produced as in cases of low velocity impact fractures.

### **2.2.2 (a) Crater formation**

Crater is produced when some glass will be flaked off at the exit side which in turn leaves a cone-shaped hole (Tryhorn, 1939). The crater is bevelling around the edge of the hole on the side opposite the origin of the bullet (Rhodes *et al.*, 1975). This bevelling is formed by the projectile pushing out the back layer of the glass as it passed through the pane. The edges of this cone are consistent with the lines of stress initially created by the impact of the bullet (Rhodes *et al.*, 1975). As bevelling is present on the exit side, more glass is lost on the exit side (Hueske, 2005). A large cone of glass will be ejected from the side opposite the impact point. This phenomenon is known as spalling (Smith, 1970). Figure 2.2 displays the crater formation on soda lime glass after penetration of a bullet.

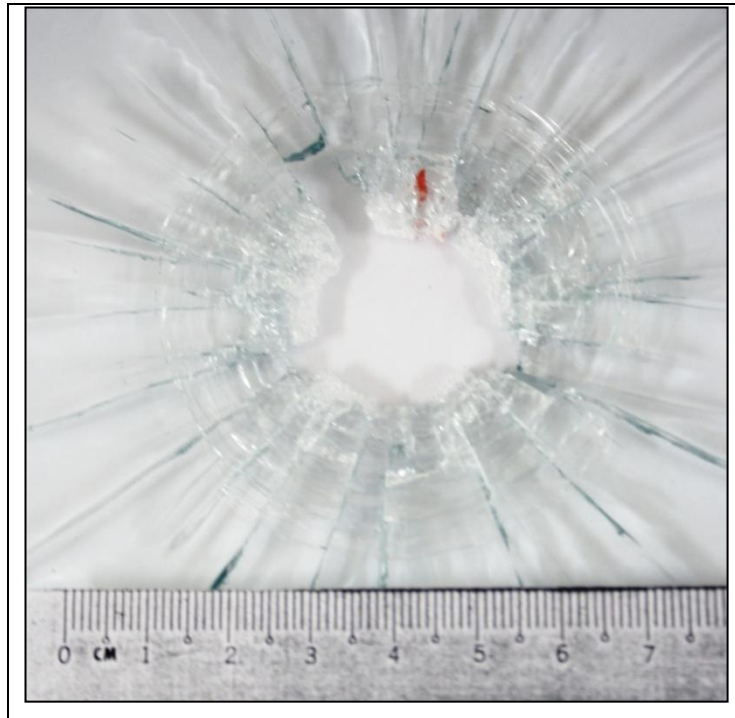


**Figure 2.2:** A crater is seen on glass on the side opposite to the direction of application of force after penetration of a bullet.

Gross (1906) and Matwejeff (1931) claimed that the origin of bullet could be determined by examining the crater formation. Matwejeff (1931) proved that direction of bullet could be determined based on the bullet hole present on the glass.

There are differences of crater morphology on soda lime silicate glass and glassy polymers. Rhodes *et al.*, (1975) studied impact fractures in glassy polymers using polymethyl methacrylate, which is typical of most acrylics found in many architectural and industrial applications in the world. In this study, they found that the bevelled edges in glassy polymers were observed to arch up and away from the centre of the hole different from the one noticed in soda lime silica glass.

Rathman (1993) established the relationship between angle of shot and the appearance of the bullet hole to automobile glass. The glass was impacted by four different calibres and at 0°, 30° and 45°. He found that the bullet holes appeared circular when the glass was impacted at 0°. As the angle of impact increased, the bullet hole became more elongated. Furthermore, the size of the bullet hole in glass was not directly proportional to the size of calibre, but was dependent on the amount of damage the bullet underwent.

Turfitt (1940) claimed that a symmetrical chamfering was produced around the exit side of bullet holes in shots fired normal to the pane. In shots fired at the glass from an angle less than 90°, the offset exit side chamfering was observed. If shots fired at right angle, more chamfering were produced on the left side and vice versa (cited by McJunkins and Thornton, 1973).

### **2.2.2 (b) Fracture pattern**

Fracture pattern induced by bullet impact produced a more complicated pattern than in low velocity impact (Brajer *et al.*, 2003). The patterns produced are dependent on the type of glass either flat glass, laminated glass, or tempered glass. They are also dependent upon the type of projectile, angle of shot, velocity of bullet, and shape of the bullet. A soft bullet (BR4) and a hard penetrating bullet (BR7) produced different fragmentation on soda lime glass (Brajer *et al.*, 2003). BR4 with a flat end crashed on the float glass target 100 x 100 x 10 mm<sup>3</sup> and were stopped.

Bullet impact damage and trajectory through laminated automobile windshield glass studied by Rathman (1993). He noted that the impact damages produced by two different calibre types, .22 calibre and 9 mm FMJ Luger showed similarities. He attributed the similarities to the more deformation of the .22 calibre producing larger hole and imparted more energy to the glass resulting in more concentric fractures. Low velocity bullets imparted much of their energy to the glass and produced more concentric and fewer radial cracks.

These observations were also recorded by Kaur (2005). She found that the fracture caused by the pistol ammunition showed short and jagged radial cracks. The presence of jagged radial cracks enabled the glass fracture induced by pistol to be physically fitted together. Rathman (1993) while studying bullet impacts in tempered glass noted that the radial cracks travelled outward from impact to the edge of the glass unlike those in windshields using laminated glass where they extended only a short distance.

The impact damage resistance of glass is determined by a combination of factors. These included not only the projectile and firearm, but also the target itself. Jauhari *et al.*, (1974) conducted measurements of the striking and remaining velocities of bullets fired from several of firearm- cartridge combinations through various thicknesses of window glass plates that ranged from 2 mm to 26 mm. The purpose of this study was to determine the wounding capability of bullets after they perforated glass targets. They observed that for glass plates of thickness 2, 3, 5.5 and 6.5 mm (laminated) the remaining velocities were much higher than the minima prescribed for the penetration of human bone and skin.

As percentage loss of velocity increased with increased glass thickness, the impulse transmitted, pressure on impact and retardation factor also increased. All these parameters were dependent upon the firearm, age and type of ammunition and target combination. It was concluded that all the four impact parameters were directly proportional to the thickness of the windowpane (Waghmare *et al.*, 2003).

More recently, the fracture patterns observed in bullet resistant glass panel laminates were reported (Ahearn *et al.*, 2006). The exterior layers of this type of glass are soda lime silicate float glass and a polymer is sandwiched between the outer glass layers. The laminated glass was impacted at high velocities by a .30 calibre flat nose projectile. Testing has been completed through a sequence of increasing projectile velocities from approximately 50 m/s to a projectile velocity 300 m/s for complete penetration of glass panels.

From the experiments, they found that the evolution of damage of laminated safety glass was increasing as velocity of projectile was increased. At lower impact velocities, the centre of impact was surrounded by a spalled region, accompanied by numerous radial and circumferential cracks outside of the spalling area (Bradt *et al.*, 2003). A continued development of cracks in the glass panel occurred at high velocity impacts. Many large circumferential cracks and spalled region occurred to the front glass plate due to extensive damage to the back side of the glass (Bradt *et al.*, 2003).

Wing crack is a thick crack which is inclined at 45° to glass surface and appears outside of the circumferential cracks in the front glass plate. It is a form of shear crack produced from a reaction to the reflected stress waves from the glass panel edges. As the velocity of projectile was increased, the density of wing cracks also increased; the diameter of perforation hole also increased as well although the diameter of spalled damaged region decreased (Bradt *et al.*, 2003).

### **2.2.2 (c) Sequence of shots**

Other than the type or direction of force applied to the glass, sequence of shots has become increasingly important in criminal investigations. A forensic scientist maybe requested to determine the order of shots from the glass fracture in the case which involved multiple shots. This is however easier in case of flat glass, as the fractures caused by the subsequent firing will be stopped by the preceding fractures. Figure 2.3 shows the sequence of shots on 2 mm thickness of soda lime glass caused by .38 in. Special calibres fired from a revolver.

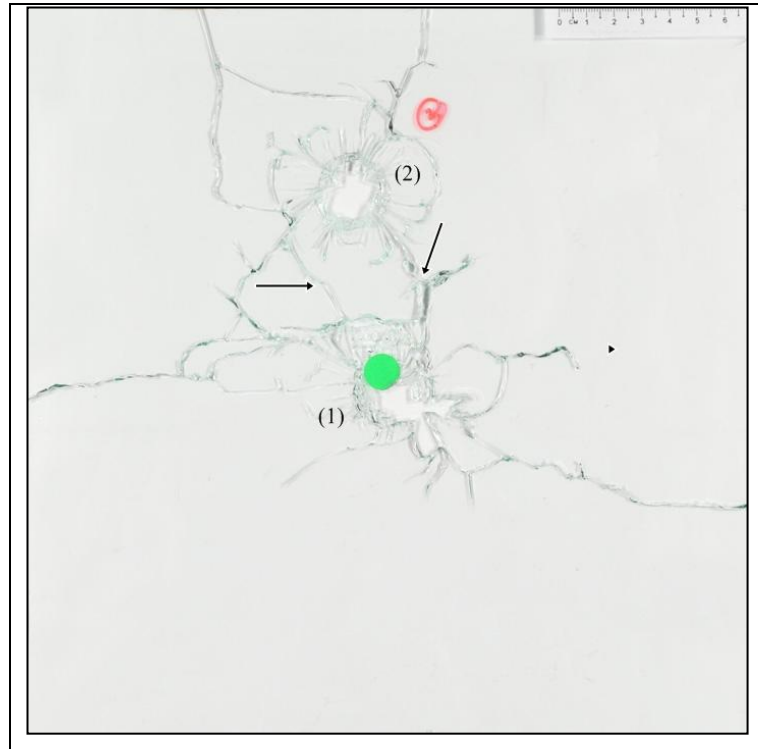


**Figure 2.3:** Fracture patterns caused by shots on 2 mm thickness of soda lime glass caused by .38 in. Special calibre. The arrows indicate the stopping of radial fracture 2 by the fracture 1. The fracture 1 was produced first.

Haag (2004) established the sequence of shots through tempered glass. The sequence of shots was based on the glass fracture patterns and also a careful examination of the recovered bullets. The first projectile to strike and perforate the glass produced numerous short radial fractures around the margin of the bullet hole on the exit side; these radial fractures turned with the diced pattern of square and rectangular pieces of glass. All subsequent shots through this diced glass produced damage to a relatively confined area because of the pre-existing cracks from the first shot.

A few studies have been carried out to estimate the shooting distance from deformation of the recovered bullets (Ben-Tovim, 1993; Fackler *et al.*, 1987) and the effect of tempered glass on bullet trajectory (Rathman, 1993; Thornton and Cashman, 1986).

## **2.3 Glass Fracture Surface Markings**

Analysis of glass fracture surfaces provides important information regarding the nature and magnitude of the stress that caused the breakage. The markings that are present on the fracture surface show the direction of propagation of the fractures (Kepple and Wasylyk, 1994). Fracture surface will be rich with fracture markings if the stress is great in the part at fracture, hence produces more stored energy and more markings will be produced. There are four types of fracture surface features: mirror, mist, rib marks and hackles (Gupta, 1994; Kepple and Wasylyk, 1994).

### **2.3.1 Mirror**

Figure 2.4 shows the formation of mirror region on fracture surface of a 5 mm thickness glass caused by 9 mm Luger FMJ fired from G-Lock pistol. Mirror is the smooth region which reflects light specularly where a crack radiates outwards from fracture origin for some distance and in a period of a microsecond. Mirror is the first type of surface of crack propagation to be formed (Ruggero, 2003; Hull, 1999; McJunkins and Thornton, 1973). No markings are produced within mirror region until the crack accelerates from zero velocity to terminal velocity, where mirror-mist markings are formed. The size of the mirror may be used to estimate the magnitude of the fracture stress (Wünsche *et al.*, 1997; Chandan *et al.*, 1994).

### 2.3.2 Mist

Mist is a region that consists of small radial ridges surrounding the mirror zone (Gupta, 1994) (Figure 2.4). Mist is a transition region between the mirror and hackle region (Chandan *et al.*, 1994). The rougher surfaces in the mist region causes a dull and no reflective appearance on the fracture surface (Mecholsky *et al.*, 2002; Kepple and Wasyluk, 1994).

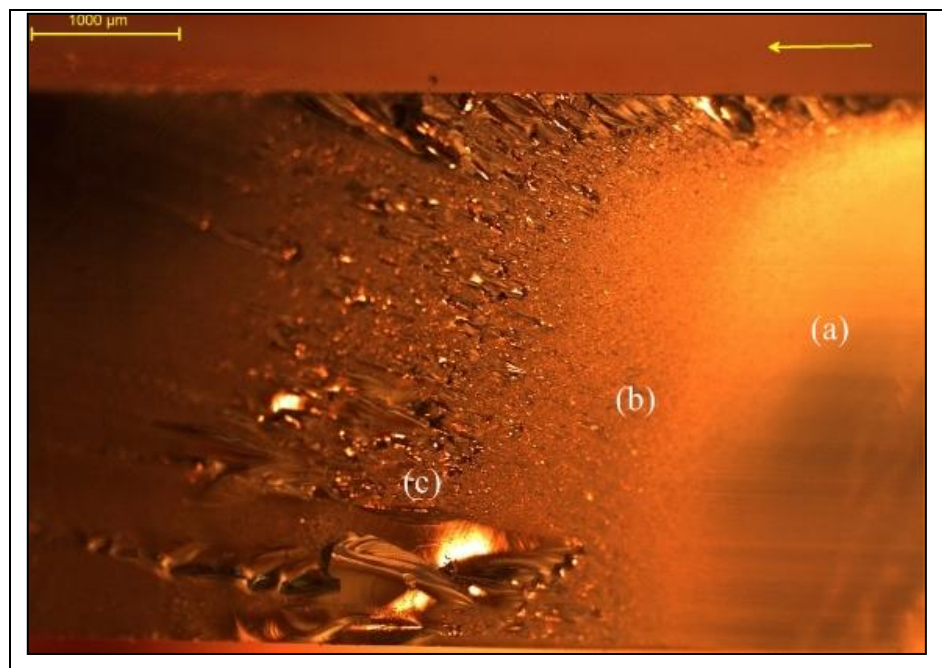


**Figure 2.4:** (a) Mirror, (b) Mist, (c) Hackle regions on the fracture surface on a 5 mm thick glass, 16 ×.

The glass was shot by 9 mm Luger FMJ calibre fired from a G-lock pistol (Refer Section 2.3.1).

### 2.3.3 Rib marks

Rib marks are commonly seen as the curved shell- like fractures that travel across the edge of the broken glass. Rib marks are the most important marks in determining the direction of the force, using the 4R rule. The 4R rule states that “**R**ib marks on **R**adial cracks are at **R**ight angles to the **R**everse side” (Koons *et al.*, 2002). Figure 2.5 illustrates the rib marks formation on radial and concentric surfaces of glass panes caused by 7.65 mm FMJ calibres shot from Walther 7.65 mm pistol.

On radial cracks, the rib marks begin almost parallel to one side, perpendicular to the far surface and curving toward the near surface of the glass. In other words, rib marks are perpendicular to the opposite side of impact. Rib marks on concentric cracks also have similar appearance as those on radial cracks. However, rib marks on concentric cracks appear perpendicular to the near surface and curving toward the far surface of the glass. Hence, rib marks on concentric cracks are at right angle to the side of impact (Koons *et al.*, 2002).

Matwejeff, (1931) concluded that orientations of the rib marks were due to the free surface upon which the fracture crack originated. It was part of the fracture process, as no rib marks were present on the glass panes after cut by glass cutter (Matwejeff, 1931).

The direction of force for bullet holes in tempered glass however could be difficult, as no rib marks on the edges of radial fractures would be present around the hole caused by the strike. Further cone fracturing might also be very subtle and this alone should be relied on for direction determination (Haag, 2004)

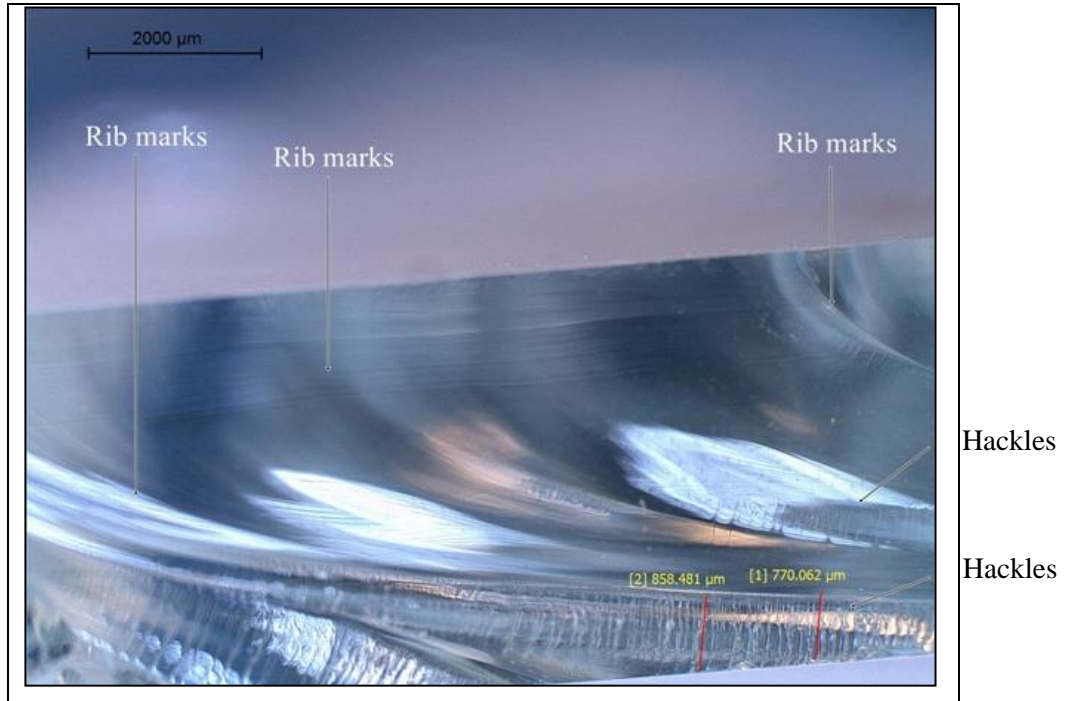


**Figure 2.5 (a):** Curved rib marks on radial cracks on a broken glass caused by 7.65 mm FMJ calibre shot from Walther 7.65 mm pistol. Also note the fine hackle marks perpendicular to the rib marks and on the side of impact,  $7.1\times$ . The arrow shows the direction of force.

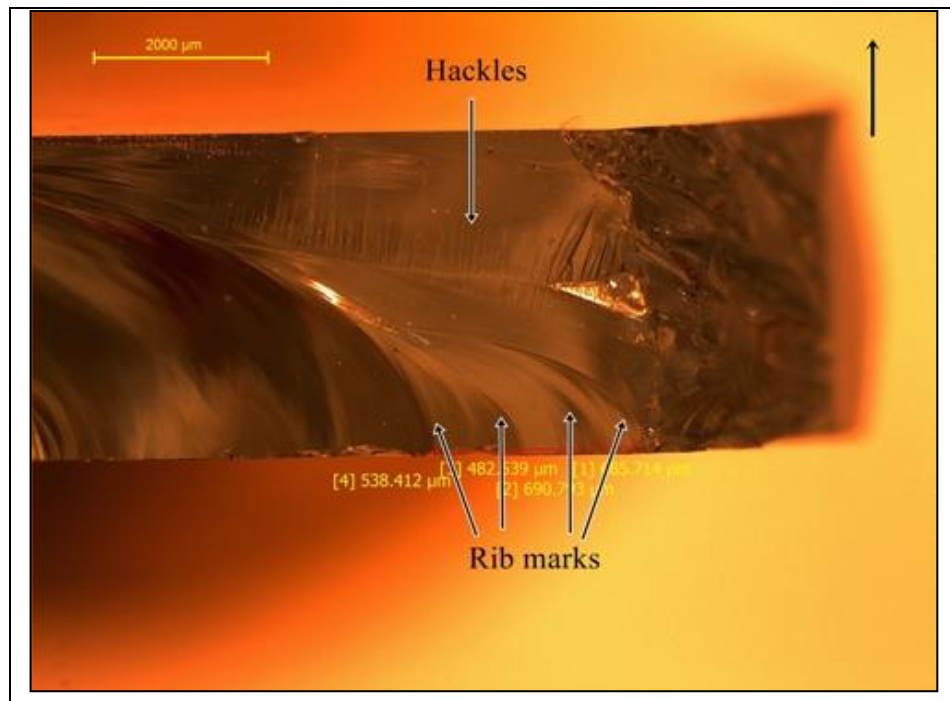


**Figure 2.5 (b):** Rib marks on concentric cracks of a glass fracture caused by 7.65 mm FMJ calibre fired from Walther 7.65 mm pistol,  $7.1\times$ . The arrow shows the direction of force.

#### **2.3.4 Hackle marks**

In low and high velocity impacts, other than rib marks, small and straight lines may be present perpendicular to the rib marks. These lines are known as hackle marks. Figures 2.6 show the hackles formation on radial surfaces caused by low velocity (Figure 2.6 (a)) and high velocity impacts (Figure 2.6 (b)). These marks occur parallel to the direction of fracture propagation (Pan *et al.*, 1989). Hackle marks on fracture surfaces were caused during a high shearing stress fracture (O'Hara and Osterberg, 1949, cited by McJunkins and Thornton, 1973). In some circumstances where rib marks are absent, hackle marks can be helpful in determining the direction of force (McJunkins and Thornton, 1973).

Hackles on the cross section in the case of fractures shot by pistol were very fine and closely spaced. However, the hackles on the cross section of glass caused by revolver were coarse and widely separated (Kaur, 2005).

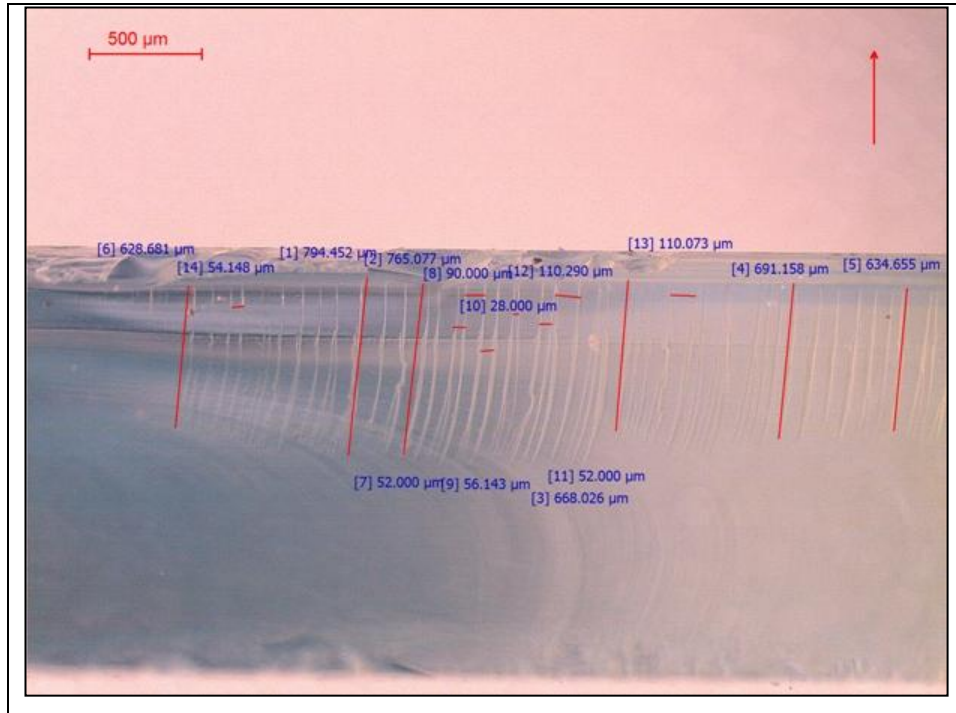


**Figure 2.6 (a):** Hackle marks on a radial crack surface produced by low velocity impact (3.10 m/ s), 32 ×. The arrow shows the direction of force.



**Figure 2.6 (b):** Hackle marks on a radial fracture surface caused by high velocity bullet impact (200 m/ s), 32 ×. The arrow shows the direction of force.

## 2.4 Fractal Geometry

Fractal geometry is being used in many fields of material science, physics, chemistry, and engineering for an explicit, objective and automatic description of production process data (Bulpakdi *et al.*, 2009; Hotar and Novotny, 2006). Fracture is one of the processes that has been modelled using fractal geometry (Mecholsky and Freiman, 1991). A fractal object has two characteristics which are self-similarity and scale invariance. Self-similarity can be defined as one region appears statistically the same as another region at the same radial distance from the origin (Mecholsky *et al.*, 2002). While scale invariance means that two features are related to each other at two different levels of magnification through a scalar magnification constant (Mecholsky and Plaia, 1992).

The fractal dimension can be determined in a number of ways. The method used for the current study is called the box counting method. This method works by overlaying a grid of boxes of size  $d$ , and counting the number of boxes  $N(d)$  that contain part of the image over it (Hotar and Novotny, 2006). The fractal dimension  $D$  is defined as  $N(d) = d^{-D}$ .  $D$  governs the rate at which  $N$  changes with  $d$  (Dannenberg, 2002) (refer section 3.3.2 (d)).

## **CHAPTER 3**

### **MATERIALS AND METHODS**

#### **3.0 Introduction**

Experiments were conducted mainly to understand better the fracture phenomena in soda lime (float) glass under bullet impacts. The data obtained could be used for estimating the calibre and type of bullets and their impact characteristics from the fracture morphology. Furthermore, the interpretation of glass phenomena can be useful to determine the events that transpired during criminal investigations. An understanding of high momentum collisions caused by bullet strikes onto soda lime glass will also determine the basic behaviour of glass during such contacts.

The bullet shooting experiments were conducted at Police Firing Range, Malaysian Royal Police (PDRM), Cheras, Kuala Lumpur after ensuring for the safety of the shooter and other experimenters and witnesses (Appendix 2, 3, 4 and 5). A few of the preliminary experiments were conducted in the Police Firing Range Gunong, Kelantan. Experiments involving “ball drop tests” on glass involving low velocity impacts were also done. These were carried out in the Development Department, Health Campus, Universiti Sains Malaysia (Appendix 1).

### 3.1 Low Velocity Glass Target Impact experiments

The simple device (Figure 3.1) was used to produce glass fracture patterns on 2 mm and 3 mm soda lime glass panes of size 200 x 200 mm at different impact velocities. These experimental results were used to illustrate some of the glass fracture characteristics involving low velocity impacts.



**Figure 3.1:** Apparatus for ball dropping experiments.